

## THE INFLUENCE OF SYNTHESIS CONDITIONS ON THE STRUCTURAL AND REDOX PROPERTIES OF Mn-MCM-41

A. M. MANTA, D. L. CURSARU\*, S. MIHAI  
*Petroleum-Gas University of Ploiești, Romania*

Mn-MCM-41 was synthesized by hydrothermal method by using surfactants with different alkyl chain lengths. The structural properties of the synthesized catalysts have been investigated by nitrogen adsorption/desorption isotherm, UV-VIS diffuse reflectance spectroscopy, X-ray Absorption Fine Structure (XAFS), Temperature Programmed Reduction (TPR), X-ray diffraction (XRD) and transmission electron microscopy (TEM). Results indicated the successful incorporation of Mn ions in the silica matrix of MCM-41. X-ray powder diffraction exposed the hexagonal mesoporous structure for Mn-MCM-4, while the N<sub>2</sub> adsorption-desorption isotherms showed a specific average surface area of 1014 m<sup>2</sup>/g. UV-VIS spectra confirmed the presence of Mn<sup>2+</sup>/Mn<sup>3+</sup> species in the framework of the mesoporous materials, and X-Ray absorption near edge spectroscopy (XANES) and extended X-ray absorption fine structure (EXAFS) were performed to determine the oxidation state and local symmetry of transition metal ions incorporated in the MCM-41 molecular sieve.

(Received January 16, 2019; Accepted July 2, 2019)

*Keywords:* Mn-MCM-4, Hydrothermal method, XRD, XAFS, TPR

### 1. Introduction

Mesoporous molecular sieves have opened new perspectives for catalytic processes, based on novel principles. In 1969 the synthesis of an ordered mesoporous material, was recorded in literature but the remarkable properties of this material have been discovered much later on [1]. The discovery in the 1990's of MCM-41 by researchers from the Mobil Oil Corporation opened new ways for the preparation, characterization and application of mesoporous molecular sieves [2,3]. These materials present remarkable features such as: high surface area, narrow pore size distribution, flexible framework structure, which make these materials interesting for their use in different applications. Catalysts efficiency for a specific reaction depends of the design of the active sites. It was shown that the characteristics of MCM-41 are strongly affected by the synthesis conditions such as: mole ratio of the components in the synthesis solution, autoclaving time, pH, silica source, etc. [4].

One of the most important properties of MCM-41 is the pore size diameter, which can be modified independently of the chemical composition of the pore walls, by changing the carbon chain length of the organic template molecules used during synthesis. The main advantages of using MCM-41 as catalyst in different applications, are the special geometric and chemical properties. Unlike crystalline zeolites, SiO<sub>2</sub> amorphous walls of mesoporous molecular sieves allow the isomorphic substitution of silicon ions with other metal cations in the matrix without altering its structure. Highly ordered Mn-MCM-41 with the metal ions incorporated in the silica matrix has been prepared for different types of reactions (e.g. the selective oxidation reaction of ethyl benzene) [5-7]. By using the hydrothermal method with isomorphous substitution of the silica ions from the matrix of MCM-41 with ions of manganese, was possible to synthesize highly ordered Mn-MCM-41 samples with the metal ions dispersed on atomic scale in the silica matrix of the mesoporous material.

---

\* Corresponding author: dianapetre@upg-ploiesti.ro

In this work we report a systematic investigation of the properties of modified silica mesoporous materials of different pore dimensions. Nitrogen adsorption/desorption isotherms and X-ray diffraction (XRD) were used for the investigation of the surface area, structure and pore size distribution, these properties being also confirmed by TEM images. UV-VIS spectroscopy and X-ray Absorption Fine Structure is important in our investigation for determining the oxidation state and local symmetry. Temperature Programmed Reduction (TPR) was useful for determination of redox properties of synthesized materials. The effect of alkyl chain length on the Mn-MCM-41 structure are compared to the similar Mn-MCM-41 results published elsewhere [8].

## 2. Materials and experimental methods

This study presents briefly the synthesis and characterization of mesoporous sieve MCM-41 with 2 wt.% Mn loading. During the synthesis step, surfactants with different number of carbon atoms  $n=14$  and  $16$  have been used.

### 2.1. Materials

Silica sources used in the synthesis of the molecular sieve was Cab-O-Sil from Riedel-de Haen and tetramethylammonium silicate from Aldrich. The manganese source used was  $\text{MnSO}_4 \bullet \text{H}_2\text{O}$  (Aldrich). The surfactant solution was prepared by ion exchanging of different quantities of cetyl trimethyl ammonium bromide aqueous solution with ion exchange resin Amberjet 4400 (Aldrich). The pH was adjusted from the synthesis solution by using acetic acid.

### 2.2. Synthesis of Mn-MCM-41

MCM-41 was synthesized following a recipe very well described in the literature [9-12]. The silica matrix of MCM-41 has been synthesized by using surfactants with different alkyl chain length, respectively C14 and C16. The manganese ions were incorporated into the framework of the matrix by hydrothermal method, in order to synthesize a molecular sieve with 2 wt.% Mn loading. The pH was adjusted at 11.5 by adding acetic acid in the synthesis solutions. The final solution was thoroughly mixed and then poured into a recipient autoclave resistant, and placed for 6 days at  $100^\circ\text{C}$  in an autoclave. After this time, the solution was cooled at room temperature, filtered and washed with deionized water. The solid part resulted after filtration was dried for 12h at  $75^\circ\text{C}$ , and finally was calcinated at a constant heating rate of  $32^\circ/\text{h}$  to  $540^\circ\text{C}$  for 18h under He flow and kept for 5h under air at the same temperature, to remove the surfactant residue.

### 2.3. Characterization

*Temperature programmed reduction (TPR).* The stability and reducibility of the transition metal ions incorporated in the MCM-41 silica framework was assessed by temperature programmed reduction using a CHEMBET Quantachrome Instrument. TPR is a useful technique for investigating the redox properties of catalysts. Approximately 100 mg of each sample was loaded into a quartz cell and heated to  $500^\circ\text{C}$  with a constant heating rate of  $5^\circ/\text{min}$  in Ar flow, held at this temperature for 1h and subsequently cooled to room temperature. This procedure was used to clean the surface of the catalysts prior to TPR investigation. For TPR investigations, Mn-MCM-41 catalyst was heated in 5%  $\text{H}_2$  in the balance from  $50^\circ\text{C}$  to  $900^\circ\text{C}$  at  $5^\circ/\text{min}$  heating ramp. The composition of the gas stream leaving the quartz cell was monitored using a thermal conductivity detector (TCD).

*Nitrogen Physisorption.* Nitrogen adsorption-desorption isotherms were measured at 77K with a ASAP Analyzer from Micrometrics. BJH method as used to determine the pore size distribution.

*X-Ray diffraction (XRD)* was recorded on a Brooker X-Ray diffractometer ( $\text{Cu K}_\alpha$ , voltage 40 kV and 5mA intensity,  $2\theta$  range  $1-10^\circ$  at a rate  $1^\circ/\text{min}$ ).

XRD measurements allowed the determination of the pore wall thickness according to a method described in the literature [12], more than that, these investigations give the first indications about the pore structure characteristic to the MCM-41 materials.

*UV-VIS Spectroscopy.* Diffusive reflectance spectra were recorded using a JASCO V 550 spectrometer. The spectra were carried out in air at the room temperature.

*X-ray Absorption.* The results obtained by X-ray absorption of the Mn-MCM-41 samples were collected at the Mn K edge using beam line X18B, at the National Synchrotron Light Source Brookhaven National Laboratory. The spectra collected were analyzed using the IFEFFIT software.

*Transmission Electron Microscopy (TEM)* is an useful and powerful techniques to image nanoscale materials. The TEM images of Mn-MCM-41 were obtained using a Tecnai F20 200kV microscope.

### 3. Results and discussion

#### 3.1. Influence of the alkyl chain length of the surfactant on MCM-41 characteristics

TPR results exposed important information about material species, stability, reducibility and metal distribution. By TPR investigation we studied the reduction behavior of supported oxide catalysts. In Fig. 1 are depicted the TPR profiles for Mn-MCM-41 catalysts with different alkyl chain length ( $n=14$  and  $16$ ). TPR investigation for Mn-MCM-41 took place in the temperature range from  $25^{\circ}\text{C}$  to  $900^{\circ}\text{C}$ . Manganese is completely reduced after we hold the temperature constant at  $900^{\circ}\text{C}$  for 1 h. If the sample is exposed to air can be re-oxidized and can form manganese oxide at the surface of the silica walls. If we tested again the sample, we obtained different patterns compared to the first TPR run. The TPR method revealed direct interaction of transition oxide phases in the silica matrix. According to the literature the first peak in TPR pattern is attributed to the reduction of  $\text{MnO}_2$  or  $\text{Mn}_2\text{O}_3$ , while the second peak the reduction of  $\text{Mn}_3\text{O}_4$  to  $\text{MnO}$  [17]. For both manganese catalysts incorporated in mesoporous molecular sieves with different alkyl chain lengths the reduction temperature is about  $600^{\circ}\text{C}$ .

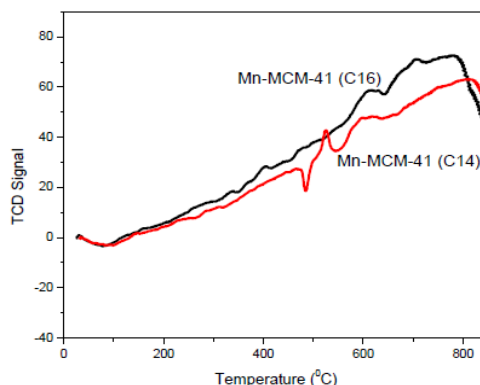


Fig. 1. Temperature programmed reduction (TPR) profiles of Mn-MCM-41 with alkyl chain length  $n=14$  and  $16$

To determine how the alkyl chain length of the surfactant affect the structure of MCM-41, the catalyst samples were characterized by nitrogen physisorption technique. Fig. 2 shows the adsorption/desorption isotherms and the distribution of the pore for as calcinated samples. The BET surface area, average pore diameter, pore volume, were determined and are presented in Table 1. It can be seen that both mesoporous materials C14 and C16 Mn-MCM-41 have uniform pore size, and the pore size decreases with the decreasing of the alkyl chain lengths. The diameter distribution of the pore can be independently changed from the chemical composition of the pore walls by changing the length of the organic template molecules during synthesis. These results are accordingly to that from the literature, being already well know that the longer surfactant chain length is, the higher relative pressure of the capillary condensation is [13]. Moreover, all samples show structural order regardless of the surfactant chain length. The higher the slope, the pores are more uniform. This can be further translated into pore size distributions obtained by using the Barret-Joyner-Halenda (BJH) method. From the pore size distribution were determined the full width at half maximum (FWHM) for each sample. It can be see that the catalysts maintained

characteristic type IV isotherms with hysteresis loop, which are the representative for mesoporous materials with uniform mesopores. Longer surfactant chain lengths result in narrower FWHM and steeper slopes for the capillary condensation. The surface area for MCM-41 and the pore volume decrease with the decreasing of the alkyl chain lengths. The sample synthesized using C16 surfactant presents a good structure comparatively with the samples using C14 surfactants in the synthesis solution.

Table 1. Surface properties of the catalysts.

Sample	Metal loading, wt. %	$S_{\text{BET}}$ ( $\text{m}^2/\text{g}$ )	Pore volume ( $\text{cm}^3/\text{g}$ )	FWHM ( $\text{\AA}$ )
C14 Mn-MCM-41	2	930	0.857	3.43
C16 Mn-MCM-41	2	1013	0.937	2.30

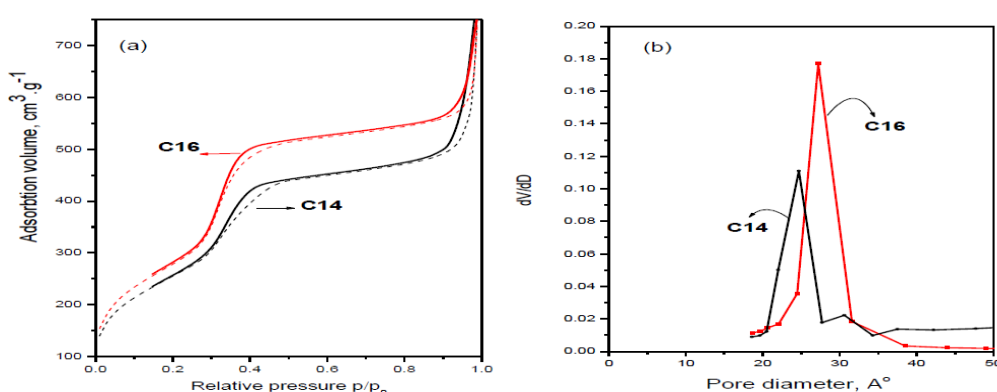


Fig. 2. Adsorption-desorption isotherms (a) and pore size distribution (b) for C14 and C16 Mn-MCM-41 samples

XRD patterns of C14 and C16 Mn-MCM-41 were taken in the  $2\theta$  range  $1-10^\circ$  at rate  $1^\circ/\text{min}$  in steps of 0.01. The XRD for both catalysts are illustrated in Fig. 3. According to XRD results, both samples present a structure characteristic for well-ordered mesoporous materials sieves, these results completing those observed for nitrogen physisorption. When recorded with a regular powder X-ray diffractometer, the XRD pattern of a well ordered MCM-41 sample usually shows one main peak which correspond to Miller index (100) and three other smaller peaks matching to higher Miller index planes (110, 200, and 210) [9].

Both samples show a sharp  $d_{100}$  reflection line in the  $2\theta$  range  $1.9-3^\circ$ , and two broad peaks at  $2\theta$  range  $3.6-5.5^\circ$  for (110) and (200) planes in MCM-41. In case of C14 and C16 Mn-MCM-41 it can be seen three peaks (100, 110, 200) by using powder at the X-ray diffractometer, indicating that the mesostructures are well developed.

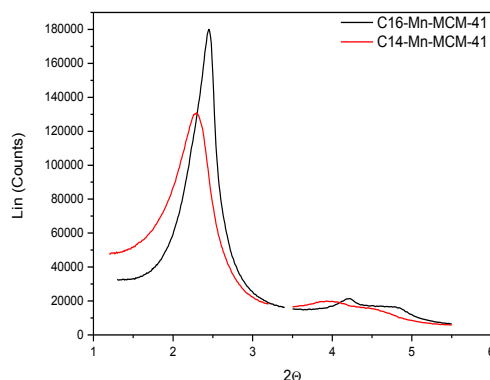


Fig. 3. XRD pattern for C14 and C16 Mn-MCM-41

In order to investigate the local environment of Mn in the MCM-41 material, samples were analyzed by UV-VIS spectroscopy and X-Ray absorption spectroscopy. Fig. 4 shows that UV-Vis spectra for Mn-MCM-41 samples present two different groups of peaks in the UV-VIS region. The UV-VIS spectra show the main absorption band centered near 250 nm and a wide band at about 500 nm which covers almost all the visible range of the spectrum. The absorption band at 500 nm is assigned to  $\text{Mn}^{2+}$  overlap, according to the literature reports, while the absorption near 250 nm is associated with  $\text{O}^{2-} \rightarrow \text{Mn}^{3+}$  charge transfer transition [17-19]. The sensitivities of the band at 250 and 500 nm may be different, and thus the intensities of these bands cannot be used to evaluate the ratio  $\text{Mn}^{2+} / \text{Mn}^{3+}$  in the samples. For both samples it was observed the same allure of the spectra, this indicating that the both types of manganese species coexist in the sample, independently of the length of the alkyl chain.

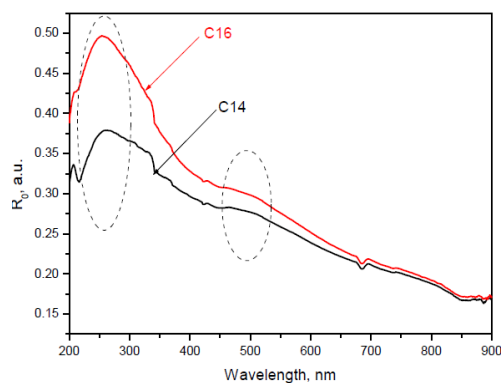


Fig. 4. UV-VIS spectra of C14 and C16 Mn-MCM-41

For X-ray absorption spectra we used the X18B beam line at the National Synchrotron Light Source, Brookhaven National Laboratory. The spectra were obtained at the Mn K edge (6535 eV) at room temperature. X-Ray absorption spectroscopy is a technique based on the absorption of X-rays and extraction of photoelectrons that are scattered by neighboring atoms [14]. An EXAFS spectrum shows these interference effects and can be used to obtain the oxidation state of the element as well as detailed information on the interatomic distances and the number and type of neighbors of the absorbing atoms [14]. A Fourier transform of the characteristic EXAFS function yields a radial distribution function, which gives the distance from the absorbing atoms [15]. All data was processed with the IFEFFIT software [16]. The oxidation state of Mn in the Mn-MCM-41 catalysts can be investigated in the derivative of the XANES spectra collected around the Mn K-edge, which is compared with commercially available reference materials (manganese oxides) in Fig. 5.

Mn (III) is a major component in all of the Mn incorporated MCM-41 catalysts as shown by the peak at 6547 eV characteristic of  $\text{Mn}_2\text{O}_3$ . The broad first peak in the catalyst spectra extended further to the left than in the spectra of Mn (III) oxide also suggests the presence of contributions from MnO.

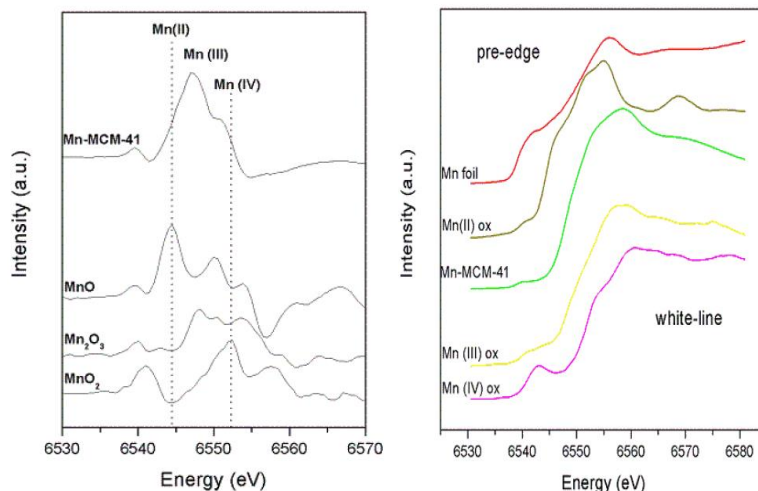


Fig. 5. X-Ray absorption spectra

Pore structure of Mn-MCM-41 samples and diameter of metallic clusters was investigated by transmission electron microscopy (TEM). By using TEM we can observe modulations in chemical identity, crystal orientation and electronic structure of the samples as the regular absorption based imaging. Images collected for our samples are presented in Fig. 6. TEM images show long range order of the synthesized materials for C14 and C16 Mn-MCM-41 with 2 wt.% Mn loading, indicating a good structure.

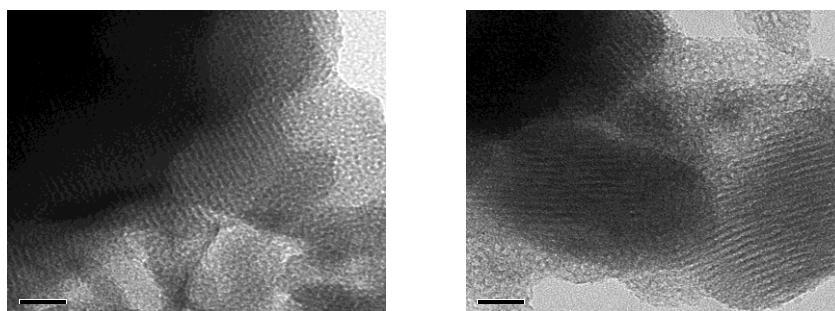


Fig. 6. TEM images for: C14-MCM-41 (left) and C16-Mn-MCM-41 (right).

#### 4. Conclusions

The mesoporous materials MCM-41 with 2 wt.% Mn loading and C14 and C16 alkyl chain length were successfully synthesized by hydrothermal method and characterized by TPR,  $\text{N}_2$  physisorption, XRD, UV-VIS, XANES and TEM. It was observed that similar to other catalysts synthesized by our group [20-23], (e.g. Co-MCM-41), the pore diameter can be controlled by changing the surfactant chain length. Mn was immobilized into mesoporous material sieves with different pore sizes and, according to different investigation techniques, present a highly ordered structure and a surface area between 930-1013  $\text{m}^2/\text{g}$ . UV-VIS spectroscopy evidenced that  $\text{Mn}^{2+}$  and  $\text{Mn}^{3+}$  in Mn-MCM-41 C14 and C16 framework are coordinated to silica surface. The

synthesized samples present high stability against reduction and can be used further in catalyzed processes for example for the selective oxidation reactions.

## References

- [1] F. Di Renzo, H. Cambon, R. Dutartre, *Micropor. Mater.* **10**, 283 (1997).
- [2] C. T. Kresge, M. E. Leonowicz, W. J. Roth, J. C. Vartuli, J. S. Beck, *Nature* **359**, 710 (1992).
- [3] J. S. Beck, J. C. Vartuli, W. J. Roth, M. E. Leonowicz, C. T. Kresge, K. D. Schmitt, C. T. W. Chu, D. H. Olson, E. W. Sheppard, S. B. McCullen, J. B. Higgins, J. L. Schlenker, *J. Am. Chem. Soc.* **114**, 10834 (1992).
- [4] Y. Yang, S. Lim, G. Du, C. Wang, D. Ciuparu, Y. Chen, G.L. Haller, *J. Phys. Chem. B.* **110**, 5927 (2006).
- [5] S. Vetrivel, A. Pandurangan, *Journal of Molecular Catalysis A* **227**, 269 (2005).
- [6] S. Gomez, L. J. Garces, J. Villegas, R. Ghosh, O. Giraldo, L. S. Suib, *Journal of Catalysis* **233**, 60 (2005).
- [7] R. K. Jha, S. Shylesh, S. S. Bhoware, A. P. Singh, *Microporous and Mesoporous materials* **95**, 154 (2006).
- [8] A. Derylo-Marczewska, W. Gac, N. Popivnyak, G. Zukocinski, S. Pasieczna, *Catalysis Today* **114**, 293 (2006).
- [9] Y. Yang, S. Lim, G. Du, Y. Chen, D. Ciuparu, L. G. Haller, *J. Phys. Chem. B.* **109**, 13237 (2005).
- [10] G. Du, S. Lim, Y. Yang, C. Wang, L. Pfefferle, G. Haller, *Applied Catalysis A* **302**, 48 (2006).
- [11] Y. Yang, S. Lim, C. Wang, G. Du, G. L. Haller, *Microporous and Mesoporous Materials* **74**, 133 (2004).
- [12] S. Lim, D. Ciuparu, Y. Chen, Y. H. Yang, L. Pfefferle, G. L. Haller, *Journal of Physical Chemistry B* **109**, 2285 (2005).
- [13] S. Lim, D. Ciuparu, C. Pak, F. Dobek, Y. Chen, D. Harding, L. Pfefferle, G. L. Haller, *J. Phys. Chem. B* **107**, 11048 (2003).
- [14] F. G. Requejo, J. M. Ramallo-Lopez, R. Rosas-Salas, J. M. Dominguez, J. A., Rodriguez, J. Y. Kim, R. Quijda, *Catalysis Today* **107-108**, 750 (2005).
- [15] D. C. Koningsberger, B. L. Mojet, G. E. van Dorssen, D. E. Ramaker, *Topics in Catalysis* **10**, 143 (2000).
- [16] A. Frenkel, C. Hills, R. G. Nuzzo, *J. Phys. Chem. B* **105**, 12689 (2001).
- [17] K. M. Parida, S. S. Dash, *Journal of Molecular Catalysis A* **306**, 54 (2009).
- [18] D. Zhao, J. Zhao, S. Zhao, W. Wang, *J. Inorg. Organomet. Polym.* **17**, 653 (2007).
- [19] N. Stamatis, K. Goundani, J. Vakros, K. Bourikas, Ch. Kordulis, *Applied Catalysis A* **325**, 322 (2007).
- [20] D. L. Cursaru, D. Enescu, D. Ciuparu, *Revista de Chimie* **62**(8), 792 (2011).
- [21] D. Matei, D. L. Cursaru, S. Mihai, *Digest Journal of Nanomaterials and Biostructures* **11**(1), 271 (2016).
- [22] D. Matei, D. Stănică-Ezeanu, D.L. Cursaru, *Digest Journal of Nanomaterials and Biostructures* **11**(4), 1343 (2016).
- [23] D. Ghiță, P. Roșca, D. Stănică-Ezeanu, *Revista de Chimie* **63**(10), 1056 (2012).